Space time distribution of afterslip following the 2003 Tokachi-oki earthquake: Implications for variations in fault zone frictional properties

S. Miyazaki,[1,2] P. Segall,[1] J. Fukuda,[3] and T. Kato[3]

Received 31 December 2003; accepted 6 February 2004; published 27 March 2004.

[1] GPS time series following the September 25, 2003 (UT) Tokachi-oki earthquake ($M_W \sim 8.0$) reveal significant deformation. We use the Network Inversion Filter to invert for the spatial and temporal evolution of afterslip in the 30 days following the earthquake. Afterslip is concentrated adjacent to the coseismic rupture zone, between the 2003 rupture and the inferred source regions of the 1968 Tokachi-oki and the 1973 Nemuro-oki earthquakes. The inversion shows a rapid decay of slip-rate in the 2003 rupture zone, with slower deceleration in the surrounding regions. The stress-velocity paths for the afterslip regions approximately follow $d\tau/d\ \ln(v) \sim 0.6$ MPa, suggestive of steady-state velocity strengthening friction. The complementary spatial pattern of coseismic rupture and afterslip may indicate along strike spatial variations of frictional properties, although other interpretations can not be ruled out. *INDEX TERMS:* 1206 Geodesy and Gravity: Crustal movements—interplate (8155); 1242 Geodesy and Gravity: Seismic deformations (7205); 1243 Geodesy and Gravity: Space geodetic surveys; 7215 Seismology: Earthquake parameters; 8150 Tectonophysics: Plate boundary—general (3040). **Citation:** Miyazaki, S., P. Segall, J. Fukuda, and T. Kato (2004), Space time distribution of afterslip following the 2003 Tokachi-oki earthquake: Implications for variations in fault zone frictional properties, *Geophys. Res. Lett.*, *31*, L06623, doi:10.1029/2003GL019410.

1. Introduction

[2] The Kurile-Japan Trench is the site of numerous large thrust earthquakes due to the subduction of the Pacific Plate beneath northeast Japan at rates of 8 ~ 9 cm/yr [e.g., *DeMets et al.*, 1990]. An M ~ 8 thrust earthquake, the 2003 Tokachi-oki earthquake, occurred off the Tokachi area, southernmost Hokkaido (Figure 1) at 19:50 on September 25, 2003 (UT). The rupture zone coincides with the source region of the 1952 Tokachi-oki earthquake (M ~ 8.2) [*Yamanaka and Kikuchi*, 2003]. The 1968 Tokachi-oki earthquake (M ~ 7.9) and the 1973 Nemuro-oki earthquake (M ~ 7.4) occurred to the southwest and northeast, respectively (Figure 1). However, it has not been clear if the fault between the 2003 and 1973 ruptures slipped in the 1952 event.

[3] Y. Yamanaka and M. Kikuchi [2004], hereinafter referred to as *Yamanaka and Kikuchi* [2004] suggest that large earthquakes along the Kurile-Japan Trench occur at fixed asperities. This implies that along the remainder of the plate interface stress is released by aseismic slip. Yet the plate interface is inferred to be strongly coupled throughout the Kurile Trench from analysis of interseismic GPS data [e.g., *Ito et al.*, 2000]. Taken together, this evidence suggests that slip in "non-asperity" areas occurs by postseismic deformation or transient slip events.

[4] Analysis of postseismic deformation following the nearby 1994 Sanriku-haruka-oki earthquake found that: 1) the net moment in the first year of afterslip equaled the coseismic moment, and 2) afterslip was concentrated downdip of the coseismic rupture [e.g., *Yagi et al.*, 2003]. The latter observation is presumed to reflect variations in physical properties with depth and temperature.

[5] In this paper, we perform geodetic inversion to infer postseismic fault slip in the 30 days following the 2003

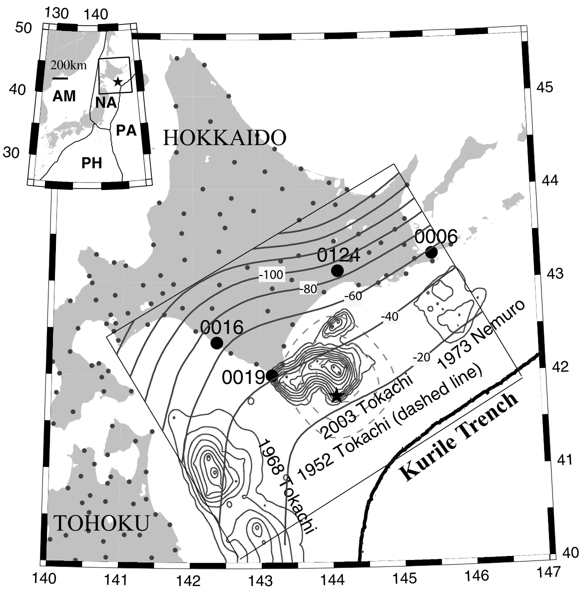

Figure 1. Tectonic setting of northeast Japan. AM, PH, PA and NA denote Amurian, Philippine Sea, Pacific and North American Plate; NEJ denotes northeast Japan. GEONET stations shown with circles; large numbered circles correspond to stations shown in Figure 2. Closed contours with 0.5m interval illustrate coseismic slip in the 1952 Tokachi (dashed lines), 1973 Nemuro, 1968 Tokachi, and 2003 Tokachi earthquakes. Epicenter of the 2003 earthquake is shown with a star. Model region is denoted with a rectangle; depth of the plate interface is contoured in kilometers. Coseismic slip contours after *Yamanaka and Kikuchi* [2004].

[1]Department of Geophysics, Stanford University, Stanford, California, USA.
[2]Visiting scientist from Earthquake Research Institute, University of Tokyo, Tokyo, Japan.
[3]Earthquake Research Institute, University of Tokyo, Tokyo, Japan.

0094-8276/04/2003GL019410$05.00

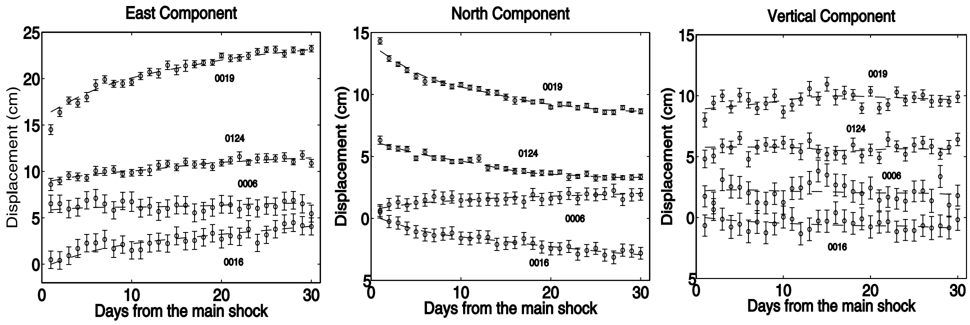

Figure 2. GPS time series at selected stations, Erimo-1 (0019), Akan (0124), Nemuro-1 (0006) and Shizunai (0016). Daily solutions are shown with open circles and 1σ error bars. Dashed line shows prediction of the modeled fault slip, excluding random benchmark motion. Reference frame corrections are subtracted from both observed and predicted data.

earthquake, using data of GPS Earth Observation Network (GEONET) operated by the Geographical Survey Institute of Japan (GSI).

2. Inversion

[6] We analyze GPS phase and pseudorange data from GEONET in Hokkaido and the northern Tohoku district by precise point positioning implemented in the GIPSY-OASIS software [*Zumberge et al.*, 1997]. Tropospheric zenith delays and gradients are modeled as random walk process with $\tau_z = 10.2$ mm/$\sqrt{\text{hr}}$ and $\tau_g = 0.3$ mm/$\sqrt{\text{hr}}$. Fiducial free orbits and network transformation parameters allow us to align the solutions to ITRF2000. Horizontal displacements of as much as 7 cm occurred in the first 30 days following the earthquake (Figure 2).

[7] We invert the GPS data for the 30 days following the mainshock (Sep. 26 to Oct. 25) to infer temporal history of afterslip on the plate interface using the Network Inversion Filter [*Segall and Matthews*, 1997; *McGuire and Segall*, 2003]. The observation equation is

$$d(t) = \int G(\mathbf{x}, \xi)\mathbf{s}(\xi)\mathbf{dS}_\xi + L(t) + Ff(t) + \epsilon(t) \qquad (1)$$

where $s(\xi)$ is slip on the fault surface S_ξ, $G(\mathbf{x}, \xi)$ are Green's functions, $L(t)$ is benchmark wobble, $Ff(t)$ is reference frame correction, and $\epsilon(t)$ is measurement error assumed to be normally distributed $\epsilon(t) \sim N(0, \sigma^2\Sigma(t))$. $\Sigma(t)$ is the covariance matrix from the GPS analysis, and σ^2 is a scaling factor to account for unmodeled errors. We adopt integrated random walk as a stochastic model for slip, random walk for benchmark wobble, and white noise for reference frame corrections. The relative weight on fitting the data versus spatial and temporal smoothing of the instantaneous slip-rate is optimized by maximum likelihood [*Segall and Matthews*, 1997].

[8] We combine the *Earthquake Research Committee* [2003] and *Katsumata et al.* [2003] models of the Kurile-Japan plate boundary. We take the model region to be 400 km in length and 360 km in width, with its northeastern edge at (145.0°E, 44.25°N), and subdivide it into 20 × 18 segments (see Figure 1). We fix the slip at the lower and upper edges to be zero, but lateral edges are kept free. Slip is expanded in two-dimensional B-spline functions of order 3 following *Yabuki and Matsu'ura* [1992].

[9] Afterslip is concentrated in regions adjacent to and along strike of the coseismic rupture zone, between the 1968, 1973, and 2003 ruptures (Figure 3 and Figure 4). In

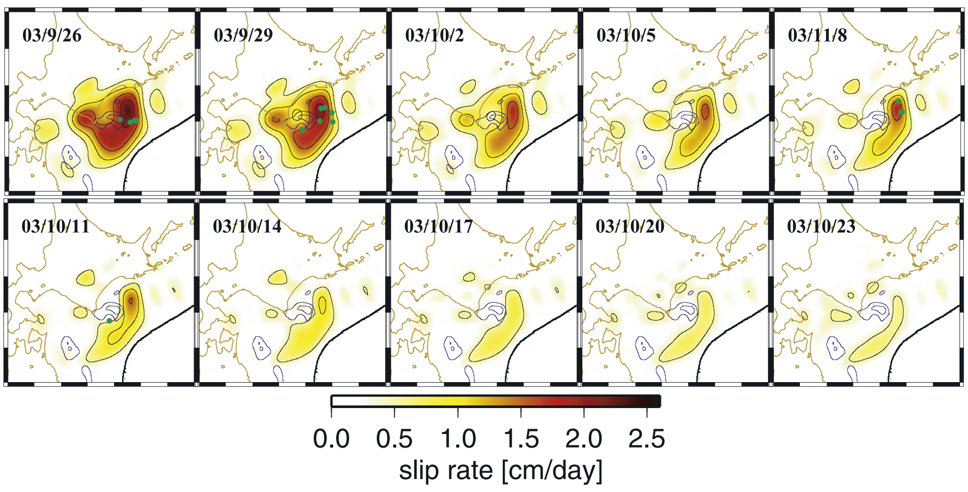

Figure 3. Spatiotemporal distribution of slip-rate, every three days, on the plate interface. Also shown are aftershocks ($M > 4$) during each time interval with one nodal plane parallel to the mainshock rupture, up to October 12, 2003 (*Ito et al.* [2004]).

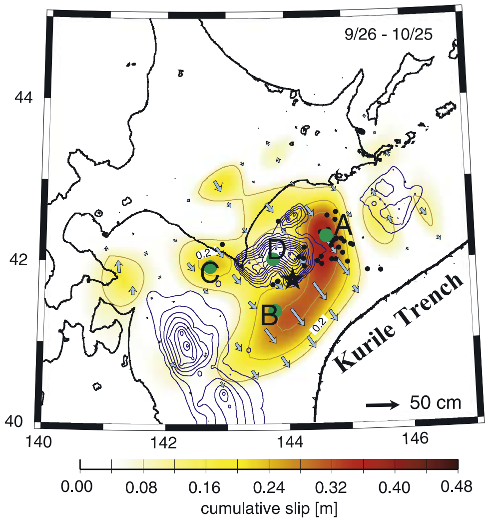

Figure 4. Cumulative slip in the 30 days following the earthquake. Arrows show the direction and magnitude of slip of the upper plate. Small circles are aftershocks ($M > 4$) with one nodal plane parallel to the mainshock rupture, up to October 12, 2003 (*Ito et al.* [2004]). Stress and slip-rate histories are shown for points A, B, C, D in Figure 6. Coseismic slip contours after *Yamanaka and Kikuchi* [2003, 2004].

spite of the smoothing imposed in the inversion, there is little afterslip in the 2003 rupture zone. Typical uncertainties are 0.15 to 0.8 cm/day for slip-rate and 0.6 to 1.2 cm for slip. We investigate the resolution of the data with a time-independent inversion[1] using the net displacement between 9/26 and 10/25. We find that slip in the coseismic rupture zone is reasonably well resolved. Slip down-dip of the rupture zone, beneath the GPS network is also well resolved. However, we cannot rule out the possibility that the estimated slip in shallower, off-shore portions of the fault is an artifact of the inversion because of poor resolution. The slip-rate history (Figure 3) shows a very rapid decay within the coseismic rupture zone and a rapid initiation of afterslip in the adjacent regions. The fault northeast of the rupture zone slipped at rates in excess of 2 cm/day on Sep. 26, and continued sliding at rates in excess of 1 cm/day for about 20 days. We also observe another locus around (142.8°E, 42°N), between the 1968 and 2003 rupture zones. The estimated moment magnitude in the first 30 days of afterslip is $M_W \sim 7.7$. The GPS time series are reasonably well fit by the model (Figure 2), with a reduced χ^2 value of 1.0.

3. Discussion

[10] No M 8 earthquakes are documented in the area immediately northeast of the 2003 hypocentral region along the Kurile Trench. It is unclear if this area slipped during the 1952 event. A notable feature of our results is that afterslip is concentrated in this region, rather than within the rupture zone. This suggests that stress in these areas is released by afterslip, rather than during earthquakes. The same behavior

[1]Auxiliary material is available at ftp://ftp.agu.org/apend/gl/2003GL019410.

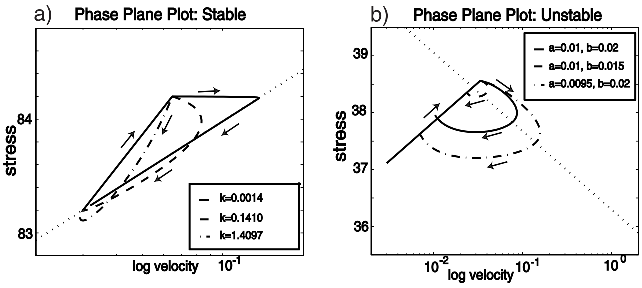

Figure 5. Predicted stress-log(velocity) paths for a single degree of freedom spring-slider with rate-state friction subject to an instantaneous stress step. a) velocity strengthening friction; b) velocity weakening friction. a, b are frictional parameters and k is the system stiffness. Dashed line indicates steady state frictional stress. In both cases the initial straight segment is a rapid change at constant state.

occurs southwest of the 2003 hypocentral zone. We infer that coseismic slip and afterslip occur on complementary parts of the megathrust. Most of the accumulated stress at the asperity is released during the main shock. This transfers stress to the adjacent regions, causing transient afterslip.

[11] Afterslip following the 2003 Tokachi-oki earthquake contrasts with that following the 1994 Sanriku-haruka-oki earthquake. Most of the 2003 Tokachi-oki afterslip occurs along strike, outside the rupture area; little occurs downdip of the rupture. In contrast, afterslip following the 1994 Sanriku earthquake occurred mainly downdip of the coseismic rupture [e.g., *Yagi et al.*, 2003].

[12] The inversions show limited, rapidly decaying afterslip in the region of the mainshock rupture. Afterslip in the adjacent regions is presumably driven by the mainshock stress change. There are two possibilities. First, that the adjacent regions are frictionally stable, (steady-state velocity strengthening), and incapable of nucleating earthquakes, consistent with the view of *Yamanaka and Kikuchi* [2004] of fixed asperities. The second possibility is that these segments of the fault are frictionally unstable, (steady-state velocity weakening), and capable of earthquakes, but at too low of a stress to support dynamic slip in 2003. In the first hypothesis the afterslip regions never nucleate large earthquakes; in the second they might in the future.

[13] Can we distinguish between these hypotheses? Rate-state friction predicts an instantaneous increase in slip-rate for an imposed increase in shear stress. Single degree of

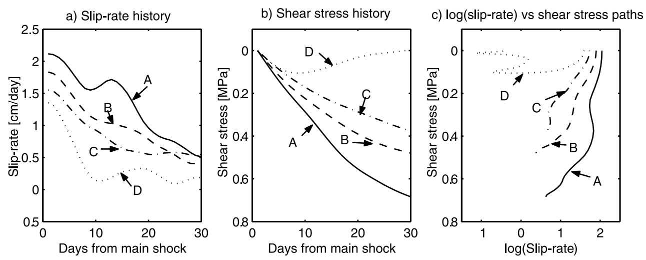

Figure 6. Slip-rate and shear stress at selected points on the fault (A, B, C, D shown in Figure 4). a) Slip-rate history; b) stress change history; c) stress change as a function of log(velocity).

freedom spring slider simulations show that for steady-state velocity strengthening behavior, slip may further accelerate before decelerating to the steady plate-rate (Figure 5a). This acceleration happens quickly and may be difficult to observe in daily deformation data. The shear stress then tends to decrease parallel to the steady-state stress-log(velocity) line [*Rice and Gu*, 1983], although the behavior varies with system stiffness.

[14] With velocity weakening friction, stress steps above a critical magnitude that depends on initial conditions and stiffness, trigger self-driven instability [*Rice and Gu*, 1983; *Gu et al.*, 1984]. Stress steps below this threshold trigger an instantaneous increase in slip-rate, possibly followed by a transient creep event (Figure 5b).

[15] To compare with these predictions we compute the change in shear stress acting on the plate boundary due to afterslip, approximating the slip distribution with numerous fine rectangular dislocations [*Okada*, 1992], and assuming a rigidity of 30 GPa and Poisson's ratio of 0.25. The stress change in the same direction as the fault slip is shown as a function of time in Figure 6b for four points on the fault shown in Figure 4. The stress within the coseismic rupture zone (D in Figure 6b) decreases briefly then reloads as the surrounding fault slips aseismically. The stress-log(velocity) path (Figure 6c) is consistent with deceleration after the mainshock. The paths for the adjoining regions (A, B, C in Figure 6c) are similar to one another, but different from that in the hypocentral region (D). This behavior appears to be more consistent with the response to a velocity strengthening fault (Figure 5a) than to a velocity weakening (Figure 5b).

[16] The observed stress-log(velocity) paths are nearly linear with slope $d\tau/d\ln(v) \sim 0.6$ MPa. If these paths parallel the steady-state frictional response [*Rice and Gu*, 1983], which should be true for sufficiently low nondimensional stiffness (Figure 5a), then these observations map the steady-state response, which we take to be $d\tau_{ss}/d\ln(v) = \sigma_{eff}(a - b)$, where a and b are frictional parameters and σ_{eff} is the effective normal stress. For a depth of ~35 km the effective normal stress would be $\sigma_{eff} \sim 600$ MPa in case of hydrostatic fluid pressure. The observations thus imply $(a - b)$ of order 0.001.

[17] The stress-log(velocity) paths for the afterslip regions suggest steady-state velocity strengthening friction on this part of the fault. Despite this, aftershocks, with thrust mechanisms and one nodal plane parallel to the plate interface, are concentrated in these areas, particularly northeast of the mainshock (Figure 4) (Y. Ito et al. [2004], hereinafter referred to as *Ito et al.* [2004]). The cumulative moment of the aftershocks, however, is more than a factor of 10 less than that measured by GPS. These observations could imply that the fault between the major ruptures exhibits dominantly stable sliding, but contains smaller patches that exhibit stick slip. It is not clear whether this interpretation can be reconciled with the inference that the megathrust is everywhere locked between great earthquakes [*Ito et al.*, 2000]. A further test of this interpretation would be to look for a possible rapid acceleration phase of afterslip in the hours after the mainshock. Alternatively our interpretation may suffer from the idealized nature of the spring-slider models, or the limited resolution in space and time of the inversion.

[18] In any case, afterslip is likely to have increased shear stress on the rupture zones of the 1973 and 1968 events. The southern half of the 1968 rupture zone slipped in the 1994 Sanriku-haruka-oki earthquake, so that the northern half of that zone is most likely to be highly stressed.

4. Conclusion

[19] We find that postseismic fault slip following the 2003 Tokachi-oki earthquake is concentrated adjacent to the coseismic rupture. The slip-rate dependence of stress is similar in the afterslip areas but differs from that in the hypocentral region. This may indicate spatial variations in frictional properties along the plate interface. Afterslip is likely to promote the occurrence of next large thrust earthquake in the source regions of the 1973 Nemuro-oki and the northern part of the 1968 Tokachi-oki earthquakes.

[20] **Acknowledgments.** We thank Y. Yamanaka for providing asperity data, Y. Ito for aftershock data, and Y. Yagi for discussion. We thank GSI for providing GPS data. We thank reviewers for comments. This study is supported by JSPS Postdoctral Fellowship for Research Abroad.

References

DeMets, C., R. Gordon, D. Argus, and S. Stein (1990), Current plate motion, *Geophys. J. Int.*, *101*, 425–478.

Earthquake Research Committee (2003), Long-term evaluation of earthquakes along the Kuril Trench (in Japanese), Headquarters for Earthquake Res. Promotion, Tokyo, 2003. (Available at http://www.jishin.go.jp/main/chousa/03_mar_chishima/index.htm)

Gu, J.-C., J. Rice, A. Ruina, and S. Tse (1984), Slip motion and stability of a single degree of freedom elastic system with rate and state dependent friction, *J. Mech. Phys. Solids*, *32*, 167–196.

Ito, Y., et al. (2004), Spatial distribution for moment tensor solutions of the 2003 Tokachi-oki earthquake (M_w = 7.9) and aftershocks, *Earth Planet. Sci.*, in press.

Ito, T., S. Yoshioka, and S. Miyazaki (2000), Interplate coupling in northeast Japan deduced from inversion analysis of GPS data, *Earth Planet. Sci. Lett.*, *176*, 117–130.

Katsumata, K., N. Wada, and M. Kasahara (2003), Newly imaged shape of the deep seismic zone within the subducting Pacific plate beneath the Hokkaido corner, Japan-Kurile arc-arc junction, *J. Geophys. Res.*, *108*(B12), 2565, doi:10.1029/2002JB002175.

McGuire, J., and P. Segall (2003), Imaging of aseismic fault slip transients recorded by dense geodetic networks, *Geophys. J. Int.*, *155*, 778–788.

Okada, Y. (1992), Internal deformation due to shear and tensile faults in a half-space, *Bull. Seismol. Soc. Am.*, *82*, 1019–1040.

Rice, J., and J.-C. Gu (1983), Earthquake aftereffects and triggered seismic phenomena, *Pure Appl. Geophys.*, *121*, 187–219.

Segall, P., and M. Matthews (1997), Time dependent inversion of geodetic data, *J. Geophys. Res.*, *102*, 391–409.

Yabuki, T., and M. Matsu'ura (1992), Geodetic data inversion using a Bayesian information criterion for spatial distribution of fault slip, *Geophys. J. Int.*, *109*, 363–375.

Yagi, Y., M. Kikuchi, and T. Nishimura (2003), Co-seismic slip, post-seismic slip, and largest aftershock associated with the 1994 Sanriku-haruka-oki, Japan, earthquake, *Geophys. Res. Lett.*, *30*(22), 2177, doi:10.1029/2003GL018189.

Yamanaka, Y., and M. Kikuchi (2004), Asperity map along the subduction zone in northeastern Japan inferred from regional seismic data, *J. Geophys. Res.*, doi:10.1029/2003JB002683, in press.

Yamanaka, Y., and M. Kikuchi (2003), Source processes of the recurrent Tokachi-oki earthquake on September 26, 2003, inferred from teleseismic body waves, *Earth Planet. Sci.*, *55*, e21–e24.

Zumberge, J., M. B. Heflin, D. C. Jefferson, M. M. Watkins, and F. H. Webb (1997), Precise point positioning for the efficient and robust analysis of GPS data from large networks, *J. Geophys. Res.*, *102*, 5017–5505.

J. Fukuda and T. Kato, Earthquake Research Institute, University of Tokyo, Tokyo, 113-0032, Japan. (fukuda@eri.u-tokyo.ac.jp; teru@eri.u-tokyo.ac.jp)

S. Miyazaki and P. Segall, Department of Geophysics, Stanford University, Stanford, CA 94304, USA. (s.miyazaki@stanford.edu; segall@stanford.edu)